Molecular Biology of the Cell
Vol. 14, 142–155, January 2003

Visualization of TGN to Endosome Trafficking through Fluorescently Labeled MPR and AP-1 in Living Cells[V]

Satoshi Waguri,*‡ Frédérique Dewitte,* Roland Le Borgne,* Yves Rouillé,* Yasuo Uchiyama,‡ Jean-François Dubremetz,* and Bernard Hoflack,*§

*Institut de Biologie, EP CNRS 525, Institut Pasteur de Lille, 59021 Lille Cedex, France; and ‡Department of Cell Biology and Neuroscience (A1), Osaka University Graduate School of Medicine, Osaka, Japan

Submitted June 13, 2002; Revised September 4, 2002; Accepted September 30, 2002
Monitoring Editor: Suzanne R. Pfeffer

We have stably expressed in HeLa cells a chimeric protein made of the green fluorescent protein (GFP) fused to the transmembrane and cytoplasmic domains of the mannose 6-phosphate/insulin like growth factor II receptor in order to study its dynamics in living cells. At steady state, the bulk of this chimeric protein (GFP-CI-MPR) localizes to the trans-Golgi network (TGN), but significant amounts are also detected in peripheral, tubulo-vesicular structures and early endosomes as well as at the plasma membrane. Time-lapse videomicroscopy shows that the GFP-CI-MPR is ubiquitously detected in tubular elements that detach from the TGN and move toward the cell periphery, sometimes breaking into smaller tubular fragments. The formation of the TGN-derived tubules is temperature dependent, requires the presence of intact microtubule and actin networks, and is regulated by the ARF-1 GTPase. The TGN-derived tubules fuse with peripheral, tubulo-vesicular structures also containing the GFP-CI-MPR. These structures are highly dynamic, fusing with each other as well as with early endosomes. Time-lapse videomicroscopy performed on HeLa cells coexpressing the CFP-CI-MPR and the AP-1 complex whose γ-subunit was fused to YFP shows that AP-1 is present not only on the TGN and peripheral CFP-CI-MPR containing structures but also on TGN-derived tubules containing the CFP-CI-MPR. The data support the notion that tubular elements can mediate MPR transport from the TGN to a peripheral, tubulo-vesicular network dynamically connected with the endocytic pathway and that the AP-1 coat may facilitate MPR sorting in the TGN and endosomes.

INTRODUCTION

The mannose 6-phosphate receptors (MPRs) are essential components for lysosome biogenesis and cellular homeostasis (Kornfeld, 1992; Ludwig *et al.*, 1995). The primary function of the cation-independent and the cation-dependent mannose 6-phosphate receptors (CI-MPR and CD-MPR) is to sort newly synthesized lysosomal enzymes from the secretory pathway for subsequent transport to endosomal/lysosomal compartments. To carry out their function, the MPRs must bind the common mannose 6-phosphate recognition marker on soluble lysosomal enzymes in the trans-Golgi network (TGN), the last sorting station of the secretory pathway, and be packaged into TGN-derived transport intermediates. After budding, these transport intermediates fuse with endosomes where the MPRs unload their bound ligands. Although the lysosomal enzymes are transported to lysosomes, the MPRs are retrieved to the TGN or occasionally to the plasma membrane. Although the precise pathways followed by the MPRs at the exit of the TGN remain to be better defined, it has become clear during the past years that the sorting of MPRs from the compartments they visit, i.e., TGN, endosomes and plasma membrane, is directed by

Article published online ahead of print. Mol. Biol. Cell 10.1091/mbc.E02–06–0338. Article and publication date are at www.molbiolcell.org/cgi/doi/10.1091/mbc.E02–06–0338.

[V] Online version of this article contains video material. Online version is available at www.molbiolcell.org.

§ Corresponding author and present address. E-mail address: hoflack@mpi-cbg.de.

† Present address: Department of Cell Biology and Neuroscience (A1), Osaka University Graduate School of Medicine, Osaka, Japan.

Abbreviations used: ARF, ADP-ribosylation factor; BFA, brefeldin A; COP, coat protein or coatomer; GFP, green fluorescent protein; MPR, mannose 6-phosphate receptor; CI-MPR, cation-independent MPR or the mannose 6-phosphate/insulin-like growth factor II receptor; VSVG, vesicular stomatitis virus G protein.

various sorting motifs present in their cytoplasmic domains (for review see Mellman, 1996). Thus, dileucine-based sorting motifs and acidic clusters are required for efficient delivery of lysosomal enzymes to lysosomes (Johnson and Kornfeld, 1992a, 1992b; Chen *et al.*, 1993; Mauxion *et al.*, 1996), tyrosine- or dileucine-based sorting motifs mediate endocytosis of MPRs (Canfield *et al.*, 1991; Johnson and Kornfeld, 1992a, 1992b), and retrieval motifs control recycling back to the TGN (Schweizer *et al.*, 1997).

Morphological studies (Geuze *et al.*, 1985; Bock *et al.*, 1997; Klumperman *et al.*, 1998) have led to the notion that MPRs are sorted from the TGN in clathrin-, AP-1–coated vesicles in a similar manner as plasma membrane receptors are packaged into endocytic clathrin-, AP-2–coated vesicles (for review see Mellman, 1996; Schmid, 1997). MPRs, their bound ligands as well as syntaxin 6, a SNARE protein involved in TGN-endosome trafficking, can be detected in vesicular profiles coated with clathrin and AP-1 assembly proteins (Geuze *et al.*, 1985; Bock *et al.*, 1997; Klumperman *et al.*, 1998) located in close vicinity of the TGN. In polarized cells, AP-1B, the epithelial specific adaptor complex that differs from the ubiquitously expressed AP-1A by exchange of its μ1A subunit by the closely related μ1B, functions by interacting with its cargo molecules and clathrin in the TGN, where it acts to sort basolateral proteins from proteins destined for the apical surface and from those selected by AP-1A for transport to endosomes and lysosomes (Folsch *et al.*, 2001). The AP-1 μ chains interact in vitro with tyrosine-based sorting motifs of several transmembrane proteins, including those contained in the MPR cytoplasmic tails (Bonifacino and Dell'Angelica, 1999) that facilitate lysosomal enzyme targeting to lysosomes (Jadot *et al.*, 1992). The translocation of cytosolic AP-1 onto membranes (Robinson and Kreis, 1992; Stamnes and Rothman, 1993; Traub *et al.*, 1993; Le Borgne *et al.*, 1996) or synthetic liposomes (Zhu *et al.*, 1999) is regulated by the small GTPase ADP-ribosylation factor (ARF)–1. Although AP-1 is located on the TGN, this coat component is also present on endocytic compartments of mammalian cells (Le Borgne *et al.*, 1996; Futter *et al.*, 1998). However, the biological significance of endosomal AP-1 has remained unclear.

More recently, a novel family of monomeric proteins known as the Golgi-localized, γ-ear–containing, ARF-binding proteins (GGAs) has been characterized (for review see (Dell'Angelica *et al.*, 2000; Robinson and Bonifacino, 2001). GGAs are made of several functional domains: a Vps27/Hrs/STAM (VHS) homology domain, an ARF binding domain, a hinge region and a carboxyl domain homologous to the ear region of the AP-1-γ subunit. Although the hinge region of GGAs binds clathrin (Puertollano *et al.*, 2001b; Zhu *et al.*, 2001), the VHS domain of GGAs interacts with the acidic cluster-dileucine–based sorting motifs present in the carboxyl-terminal domain of MPRs or sortilin, another membrane protein (Nielsen *et al.*, 2001; Puertollano *et al.*, 2001a; Takatsu *et al.*, 2001; Zhu *et al.*, 2001). Furthermore, GGA1 is present on TGN-derived transport intermediates containing CD-MPRs (Puertollano *et al.*, 2001a), clearly indicating that GGAs are involved in MPR sorting at the TGN. Whether GGAs and AP-1 function along the same or different sorting pathways remains unknown. More elusive is now the function of AP-1 in TGN sorting because the targeted disruption of the AP-1 μ1-A subunit gene in mice has suggested that AP-1 functions in the retrieval of MPRs from endosomes to the TGN (Meyer *et al.*, 2000). In yeast, AP-1 and clathrin act to recycle chitin synthase III and Tlg1p, a resident TGN/early endosome syntaxin, from the early endosome to the TGN (Valdivia *et al.*, 2002).

In this study, we have expressed chimeric proteins made of fluorescent proteins fused to the transmembrane and cytoplasmic domain of CI-MPR or to the AP-1 γ-subunit to visualize their dynamics in living cells. Time-lapse videomicroscopy indicates that the GFP-CI-MPR chimeric protein exits from the TGN via tubular elements. Their formation is controlled by the ARF-1 GTPase and depends on the presence of microtubule and actin networks. The TGN-derived transport carriers detach from the TGN, move toward the cell periphery, and then fuse with peripheral tubulo-vesicular structures that also contain the GFP-CI-MPR. These peripheral structures are highly dynamic, interacting with each other as well as with endosomes containing internalized transferrin. Two-color time-lapse microscopy indicates that YFP-AP-1 is present on these TGN-derived transport intermediates carrying the CFP-CI-MPR. This AP-1 coat remains occasionally associated, whereas the TGN-derived transport intermediates fuse with the next compartment. These results not only suggest that AP-1 may be involved in MPR transport from TGN to endosomes but also that AP-1 may function as a device to concentrate membrane proteins in selected membrane domains.

MATERIALS AND METHODS

Reagents

BFA, nocodazole, cytochalasin D, and wortmannin were purchased from Sigma Chemical Co. (St. Louis, MO).

Antibodies

The following primary antibodies were used: mouse monoclonal antibodies, SG1 (Viro Res. Inc., Rockford, IL) against varicella-zoster virus glycoprotein I, P5D4 against VSVG protein epitope (kindly provided by Dr. T. Kreis), 100.3 against γ-adaptin (Sigma Chemical Co.), rabbit polyclonal antibodies against the CI-MPR luminal domain (Ludwig *et al.*, 1991), clathrin (kindly provided by Dr. P. Mangeat, Montpellier, France), recombinant GFP (Clontech, Palo Alto, CA), and His-tagged GFP (kindly provided by Dr. Karsenti; EMBL, Heidelberg, Germany). Secondary antibodies against mouse and rabbit IgGs coupled to Texas red were purchased from Jackson ImmunoResearch Laboratories Inc. (West Grove, PA).

DNA Constructs

To produce an expression vector for the GFP-chimeric protein named pCIpreEGFP-CIMPRtail, we first introduced a signal peptide from preproglucagon to the EGFP molecule. A 1-kbp *Dde*I fragment of preproglucagon cDNA (Bell *et al.*, 1983) was subcloned into the *Xho*I site of pCIneo (Promega, Madison, WI), after Klenow treatment of the insert and the vector. The resulting pCIglu2 expression vector was first cleaved with *Xho*I, a unique site inside the prosequence, filled in with Klenow, then cleaved with *Not*I, and ligated to the EGFP cDNA fragment obtained from pEGFP-C1 (Clontech) by successive *Nco*I, Klenow, and *Not*I actions. The resulting construct was named pCIpreEGFP-C1. A PCR fragment encoding the CI-MPR transmembrane and cytoplasmic domains was generated from a mouse CI-MPR cDNA clone using the following primers: forward primer, 5′-CCCGCTCGAGCTGTTGGGGCAGTCCTC -3′, reverse primer, 5′-CGGAATTCTTAGATGTGTAAGAGGTCTTCG-3′. In-

troduction of *Xho*I and *Eco*RI sites into the forward and reverse primers, respectively, allowed the cloning of the PCR fragment into the same site of pCIpreEGFP-C1. The resulting construct, pCIpreEGFP-CIMPRtail, encodes a chimeric protein composed of the signal peptide and 21 residues from the N-terminus of the glucagon biosynthetic precursor, the complete EGFP, a linker sequence (6 residues), and the transmembrane and cytoplasmic domains of CI-MPR. The cyan version of pCIpreECFP-CIMPRtail was constructed in the same way as described above using pECFP-C1 (Clontech). To construct the GFP (or YFP)-γ adaptin fusion protein, a PCR fragment encoding the complete open reading frame of the human γ adaptin was amplified from a human brain cDNA library (Clontech) using the following primers: forward primer, 5′-CCGCTCGAGATGCCAGCCCCCTACAGATTG-3′, reverse primer, 5′-CGGTGGATCCCGTTGCCAGGACTGAGGGGGAAA-3′. It was then digested with *Xho*I and *Bam*HI and cloned into the corresponding site of the expression vector, pEGFP (or EYFP)-N1 (Clontech). The bovine ARF-1 cDNA was kindly provided by Dr. P. Chardin (Institut de Pharmacologie Moléculaire et Cellulaire, Valbonne, France) and cloned into the pGEM2 vector (Promega). The mutant ARF-1, ARF-1Q71L, was produced by oligonucleotide-directed PCR mutagenesis. All the constructs were confirmed by sequencing using the dye-terminator cycle sequencing kit (PE Applied Biosystems, Foster City, CA). pSRα-STVSVG was kindly provided by Dr. T. Nilsson (EMBL, Heidelberg, Germany) for expression of a VSVG epitope-tagged version of the rat sialyltransferase (Rabouille *et al.*, 1995). pSFFV-gpI was as reported previously (Alconada *et al.*, 1996).

Cells

HeLa cells were grown in α-MEM supplemented with 10% FCS, 2 mM glutamine, 100 U/ml penicillin, and 100 μg/ml streptomycin at 37°C in a humidified atmosphere of 5% CO_2. Cells were transiently transfected either by the calcium phosphate method (Alconada *et al.*, 1996) or using FuGENE 6 (Roche Diagnostics; Mannheim, Germany). Transient expression of ARF1-Q71L was performed using the vaccinia T7-DOTAP system as previously reported (Alconada *et al.*, 1996). For generation of stable cell lines, 40 μg of the pCIpreEGFP-CIMPRtail was linealized with *Bam*HI and transfected into HeLa cells using the calcium phosphate method. After 12–14 d of selection with G418 sulfate (Calbiochem, La Jolla, CA), 40–50 isolated colonies were picked up and checked for the expression of EGFP-fusion proteins by fluorescence microscopy, immunoprecipitation, and Western blotting.

Immunofluorescence

HeLa cells stably or transiently expressing the fluorescent CI-MPR or γ adaptin were fixed with 3% paraformaldehyde for 15 min at room temperature, and the excess paraformaldehyde was quenched by a 10-min incubation in 50 mM ammonium chloride in PBS. The cells were permeabilized with 0.1% Triton X-100 in PBS, incubated for 20 min in 10% normal goat serum in PBS, and then for 30 min with each of the antibodies diluted to working concentrations with 10% normal goat serum. They were observed with either a confocal laser scanning microscope, a LSM510 (Carl Zeiss, Jena, Germany) or an Axioplan 2 Universal Microscope (Carl Zeiss). The EGFP in the fusion protein was excited by a laser beam of 488 nm or a UV light passed through a 458-nm band-pass filter, and detected through a 515–565-nm band-pass filter. The CFP signal was excited by a laser beam of 458 nm and detected through a 475–515-nm band-pass filter set, whereas YFP was excited by a laser beam of 514-nm wavelength and detected through a 530–600-nm band-pass filter.

For labeling endosomes, human transferrin (Sigma Chemical Co.) was first labeled with Alexa594 (Molecular Probes, Inc., Eugene, OR) according to the manufacturer's instructions and then loaded with iron following the method described by Stoorvogel *et al.* (1987). After incubation with 0.1 μM transferrin-Alexa594 for various periods of time, the cells were washed and fixed for observation.

Electron Microscopy

HeLa cells stably expressing the GFP-CI-MPR chimera and transiently expressing the VSVG epitope-tagged sialyltransferase were fixed with 4% paraformaldehyde-0.05% glutaraldehyde in PBS (pH 7.4) for 90 min. After washing with 10% FCS in PBS, the cells were collected, pelleted, and infused with a 2.3 M sucrose solution containing 20% polyvinylpyrrolidone. After being frozen in liquid nitrogen, thin sections were cut with an ultramicrotome (Ultracut-E, Leica, Deerfield, IL) and mounted on nickel grids. Sections were treated with 10% FCS in PBS for 30 min at room temperature and then incubated at room temperature for 1 h with an anti-GFP polyclonal antibody (provided by Dr. Karsenti) and an anti-VSVG mAb. They were then incubated for 1 h with gold-conjugated goat anti-rabbit IgGs (5 nm colloidal gold) and goat anti-mouse IgGs (10 nm colloidal gold; Amersham Pharmacia Biotech, Piscataway, NJ). Between each step, the grids were washed in PBS/BSA. After the immunoreactions, the sections were stained, embedded in 0.3% uranyl acetate 2% methylcellulose, dried, and observed with a Philips EM420 electron microscope (Mahwah, NJ).

Time-lapse Imaging and Microscopy

To observe live-cells, we used the Bioptechs ΔTC3 controlled culture dish system (Bioptechs Inc., Butler, PA) that allows controlling accurately the microenvironment temperature. The cells expressing GFP-CI-MPR were grown on the special dishes of the system. After exchanging medium with fresh complete medium supplemented with 10 mM HEPES buffer, the cells were viewed with a Zeiss Axiovert 100 M equipped with a 63× objective lens (Plan-Apochromat; Carl Zeiss). The GFP molecules were detected with the same filter set as described above. The time-lapse recording was operated with the MetaMorph Imaging System (Universal Imaging Corporation, West Chester, PA) through a cooled CCD camera (MicroMAX 5 MHz system; Princeton Instruments, Inc., Trenton, NJ). The dynamics of GFP-CI-MPR were routinely recorded under various conditions with a 2-s of interval time and 100–250 ms of exposure time, whereas fast recordings were usually performed at a speed of three frames per second with no interval time.

To examine the BFA effects, a drop of a stock solution of the drug was added at the beginning of the recording of HeLa cells expressing GFP-CI-MPR to reach a final concentration 10 μg/ml. For other reagents, the cells were treated with nocodazole (10 μM for 60–90 min), cytochalasin D (1 μM for 30–60 min), and wortmannin (100 nM for 10–30 min) before recording.

Two-color recordings were performed on a Zeiss confocal microscopy, LSM510 with a 63× objective lens (Plan-Apochromat). The cells expressing GFP-CI-MPR were labeled with 0.1 μM transferrin-Alexa594 for 30 min at 4°C and then washed three times with a medium without transferrin-Alexa594. The dynamic interactions of both signals were recorded after warming up to 37°C for 5, 10, or 15 min. The GFP was excited by the 488 nm line of an Argon laser and detected through a 503–530-nm band-pass filter, and Alexa594 was excited by the 543 nm line of a Helium-Neon laser and detected through a 560–615 nm filter. For another color combination, plasmids encoding CFP-CI-MPR and YFP-γ adaptin were cotransfected using FuGENE 6 for ~8 h. After changing the medium, the cells were allowed to express the proteins for additional 16 h. The filter sets used for these experiments were as described above. Selected parts (about one-third to one-fourth of whole cells) were scanned with the multitrack mode at a speed of 0.5–1.5 s/frame with no interval time. The images were processed through a low pass filter to remove noises with the software in the LSM510 system.

RESULTS

To visualize the dynamics of the mannose 6-phosphate receptors in living cells, we stably expressed in HeLa cells a fusion protein made of GFP fused to the transmembrane and

cytoplasmic domains of the Man-6-P/IGF II receptor (or cation-independent mannose 6-phosphate receptor, CI-MPR). A representative clone was selected for further studies. Pulse-chase experiments indicated that the level of expression of GFP-CI-MPR was ≈3–4 times higher than that of the endogenous CI-MPR in these cells and that the two proteins had similar half-lives (unpublished data). However, the expression of the GFP-CI-MPR did not significantly affect the trafficking of the endogenous MPRs because no significant missorting of lysosomal enzymes could be detected (unpublished data). Finally, antibody uptake experiments indicated that similar amounts (up to 30% within 2 h) of GFP-CI-MPR and endogenous CI-MPR passed through the cell surface and recycled back to the TGN indicating that both proteins traffic in a similar manner (unpublished data).

Cellular Distribution of the GFP-CI-MPR

A first examination of GFP-CI-MPR–expressing HeLa cells showed that this fusion protein distributed to different intracellular compartments (Figure 1A). The bulk of the fluorescent protein (≈90%) was present in the perinuclear region where the TGN and the late endosomes are usually located. Significant amounts of GFP-CI-MPR were also detected in small tubular structures scattered throughout the cytoplasm. This fluorescence pattern was not changed after cycloheximide treatment, indicating that these small tubular structures were different from the endoplasmic reticulum (unpublished data). Using transient expression, we first introduced different TGN markers in these cells, namely the VSVG-tagged sialyltransferase (Rabouille *et al.*, 1995) and the gpI envelope glycoprotein of the varicella-zoster virus, a transmembrane protein that cycles between the TGN, the plasma membrane, and the endosomes (Alconada *et al.*, 1996). The bulk of GFP-CI-MPR present in the perinuclear region almost completely colocalized with sialyltransferase, gpI, and the endogenous CI-MPR at the fluorescence level (Figure 1, B–D). Interestingly, the GFP-CI-MPR labeled long tubular processes protruding from this perinuclear compartment in several cells. If these tubular elements could also be decorated with anti-gpI or anti–CI-MPR antibodies, they appeared to exclude the VSVG-tagged sialyltransferase. Thawed cryosections of HeLa cells expressing the GFP-CI-MPR and the VSVG-tagged sialyltransferase were also labeled with a polyclonal antibody against GFP and a mAb against the VSVG-epitope followed by colloidal gold. Electron microscopy (Figure 1F) shows that the bulk of the GFP-CI-MPR was found in tubular vesicular structures reminiscent of the TGN, located in the close vicinity of the Golgi stacks containing the sialyltransferase. No significant labeling was detected over late endocytic compartments (unpublished data). We also internalized fluorescently labeled transferrin for 10 min at 37°C to identify early endocytic compartments. The internalized transferrin could be detected in ≈30% of the peripheral, GFP-labeled structures (Figure 1E). Altogether, these data indicate that the bulk of the GFP-CI-MPR localizes to the TGN and that small but significant amounts are present in early endosomes containing endocytosed transferrin as well as in peripheral structures devoid of this marker.

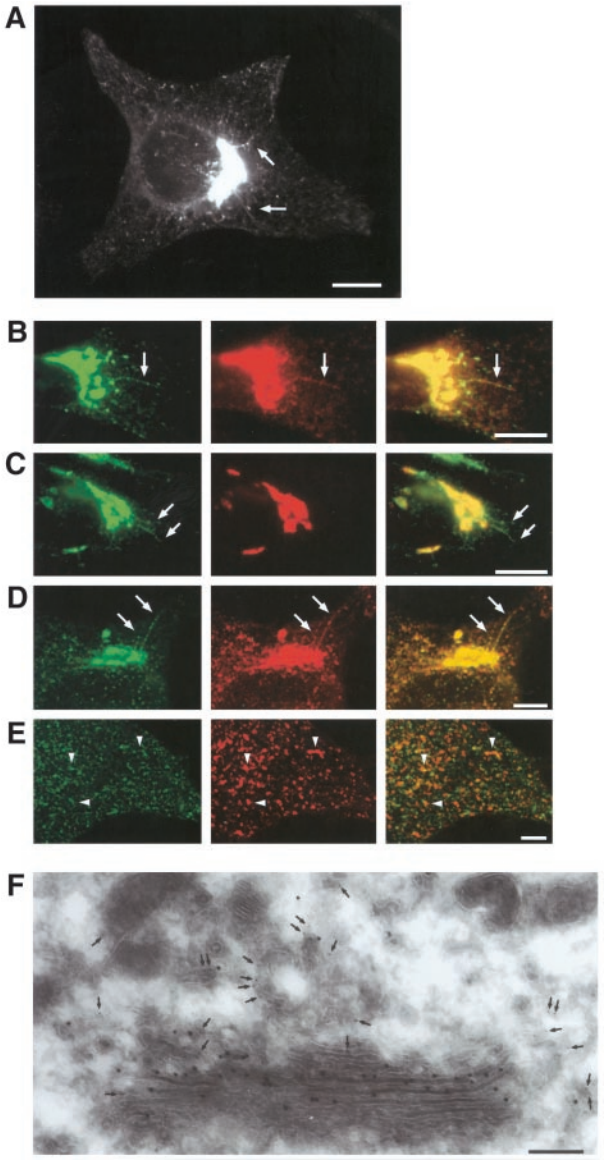

Figure 1. Distribution of the GFP-CI-MPR chimeric protein. (A) HeLa cells stably expressing GFP-CI-MPR were fixed and examined by fluorescence microscopy. (B and C) HeLa cells stably expressing GFP-CI-MPR (green) and expressing transiently markers of the trans-Golgi network, namely gpI (B) or a VSVG epitope-tagged sialyltransferase (ST; C). The cells were fixed and immunolabeled with a mAb against the VSVG epitope or the SG1 anti-gpI mAb followed by a Texas Red–conjugated goat anti-mouse antibody (red). (D) HeLa cells expressing GFP-CI-MPR (green) were fixed and labeled with a polyclonal antibody against the luminal domain of CI-MPR (red). (E) These cells were also allowed to internalize Alexa594-labeled transferrin for 10 min at 37°C (Tf-Alexa594; E). (B–D) The GFP signal in the Golgi region; (E) GFP signal in the periphery of the cell. Merged images are presented in the right column. Arrows indicate long tubules emanating from the perinuclear region. Arrowheads in E indicate examples of the overlap between both signals. Bars, 10 μm. (F) Thawed thin sections of HeLa cells stably expressing GFP-CI-MPR and transiently expressing the VSVG epitope-tagged sialyltransferase were double immunolabeled with a polyclonal anti-GFP antibody (5 nm colloidal gold, arrow) and a monoclonal anti-VSVG antibody (10 nm colloidal gold). Bar, 0.2 μm.

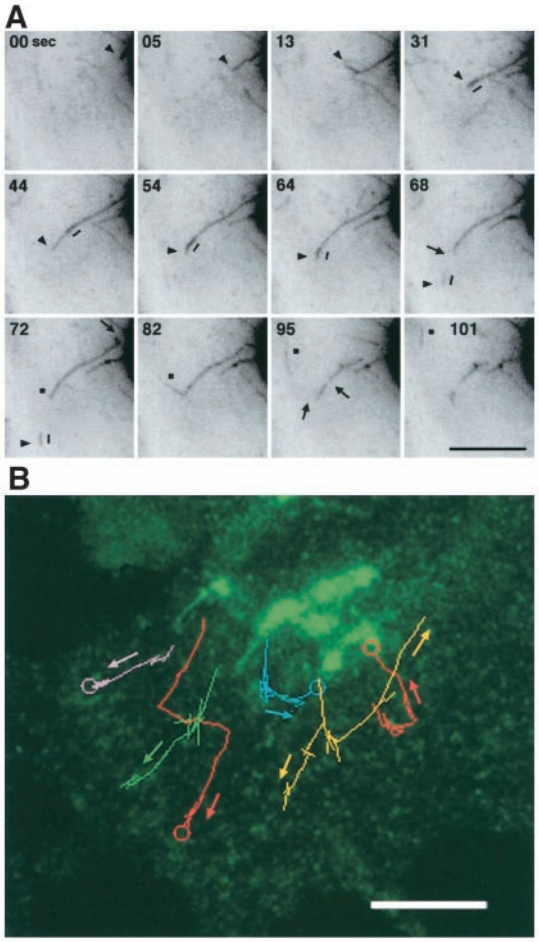

Figure 2. Formation of tubular elements from the TGN. (A) HeLa cells expressing the GFP-CI-MPR were examined by videomicroscopy. Images were taken at 2-s time intervals. Inverted images at the indicated time intervals are displayed. Arrowheads or squares indicate the tips of TGN-tubules, the arrows indicate the detachment of long tubular elements from the TGN and the breaking points into smaller tubular elements. The short line indicates a more intense GFP labeling that moves along the tubule toward the tip and then detaches from it. (B) Movement of TGN-derived tubules toward the cell periphery. Images were collected at 1-s intervals for 1 min. Paths of different TGN-derived tubules were traced as colored lines. The circles indicate fusion with GFP-CI-MPR containing structures. Bars, 10 μm.

Dynamics of GFP-CI-MPR in the TGN

Using time-lapse videomicroscopy, we then visualized the dynamics of the GFP-CI-MPR located in the TGN. Figures 2A and 4A illustrates that the GFP-CI-MPR is sorted from the TGN in tubular structures of various lengths. These tubules are highly dynamic elements. With time, they elongated with an average speed of $\approx$0.9 μm/s, sometimes forming branched structures at the tip. Smaller tubular fragments could detach from the growing tubules and moved toward the cell periphery with an average speed of $\approx$0.9 μm/s (Figure 2B). These long tubular processes, which occasionally reached a length of 10 μm, could detach from the TGN and break into several smaller tubular fragments that moved toward the cell periphery with an average speed of $\approx$0.9 μm/s, most likely along microtubules. The statistical analysis of the dynamic state of these TGN-connected tubules (Table 1) shows that $\approx$4 tubular elements with an average length of 6 μm could form within 2 min. Tubule formation, frequently occurring on the same restricted domains of the TGN, usually takes place with an average duration time of 20 s.

The dynamic state of the tubular elements depends on several factors (Table 1). First, these events are temperature dependent. When GFP-CI-MPR–expressing cells were maintained at 20°C, a temperature known to drastically reduce protein sorting in the TGN, only few tubular elements ($\approx$1 per 2 min) with a shorter length ($\approx$2.8 μm) were seen. Under those conditions, the speed of elongation was also decreased (0.5 μm/s). Second, tubule formation requires the presence of cytoskeleton elements. This could be monitored when GFP-CI-MPR–expressing HeLa cells were treated with nocodazole, a drug known to destabilize microtubules. In nocodazole-treated cells, the Golgi rapidly fragmented into smaller elements scattered in the cytoplasm as previously described (Scheel *et al.*, 1990). However, AP-1 and clathrin remained in a large part associated to these scattered elements (unpublished data). GFP-labeled tubules were unable to grow from these scattered Golgi elements. In a similar manner, tubule formation was almost completely abolished when cells were pretreated with cytochalasin D, a drug destabilizing the actin network. Cytochalasin D did not affect the distribution of coat components such as AP-1 and clathrin (unpublished data). Altogether, these results show that tubule formation depends on the temperature, requires the presence of both an intact microtubule network and actin filaments.

The ARF-1 GTPase, but not Wortmannin-sensitive PI-3 kinases, Regulates TGN-derived Tubule Formation

Several studies have now shown that the ARF-1 GTPase regulates the translocation onto membranes of AP-1 and GGAs, two coat components involved in MPR trafficking (Stamnes and Rothman, 1993; Traub *et al.*, 1993; Le Borgne *et al.*, 1996; Zhu *et al.*, 1998; Meyer *et al.*, 2000; Nielsen *et al.*, 2001; Puertollano *et al.*, 2001a; Takatsu *et al.*, 2001; Zhu *et al.*, 2001). We therefore expressed ARF-1Q71L, a mutant impaired in GTP hydrolysis, in GFP-CI-MPR–expressing HeLa cells using a vaccinia recombinant virus. Under those conditions, the Golgi appeared as a cluster of smaller, GFP-labeled elements, still concentrated in the perinuclear region (unpublished data). As illustrated in Table 1, no tubule could form from these GFP-labeled compartments, indicating that GTP hydrolysis by ARF-1 regulates tubule formation.

In contrast, brefeldin A (BFA), which blocks the translocation of ARF-1 on membranes (Klausner *et al.*, 1992) and the subsequent binding of AP-1 (Robinson and Kreis, 1992; Wong and Brodsky, 1992) and GGAs (Boman *et al.*, 2000; Dell'Angelica *et al.*, 2000; Hirst *et al.*, 2000), results in the formation of a tubular network containing both TGN and endosomal markers (Lippincott-Schwartz *et al.*, 1991). We then incubated the GFP-CI-MPR–expressing HeLa cells with

Table 1. Dynamics of TGN-tubules

Variables	Number of tubules in a 2-min interval	Speed (μm/sec)	Length (μm)	Range of duration (sec)
Normal conditions	3.9 ± 1.8 (n = 20)	0.9 ± 0.2 (n = 58)	6.3 ± 3.0 (n = 57)	21.4 ± 17.5 (n = 57)
20°C	1.1 ± 1.5 (n = 14)	0.5 ± 0.2 (n = 9)	2.8 ± 1.0 (n = 16)	23.0 ± 15.7 (n = 13)
Nocodazole	n.d.			
Cytochalasin D	0.2 ± 0.4 (n = 10)			
BFA	11.1 ± 3.7 (n = 20)	0.9 ± 0.3 (n = 75)	14.4* ± 5.1 (n = 16)	95.6* ± 52.0 (n = 52)
ARF-1Q71L	n.d.			
Wortmannin	4.0 ± 2.5 (n = 18)	0.8 ± 0.3 (n = 46)	5.1 ± 2.6 (n = 54)	21.1 ± 16.5 (n = 50)

TGN-tubules in GFP-CI-MPR-expressing cells were analyzed under the conditions indicated (for more details, see MATERIALS AND METHODS and RESULTS). Values correspond to means ± standard deviation. n in the columns "Number of tubules" and "Speed" indicates the number of cells and growing events of tubules, respectively, while n in "Length" and "Range of duration" columns indicates the number of tubules observed. The values marked with an asterisk are underestimated due to limitations of the time and frame sizes in the different recording conditions. n.d., tubules were not detected.

BFA. The dynamics of tubules emanating from the TGN rapidly changed within 1–3 min after addition of BFA (Figure 3), and after 10 min, BFA treatment resulted in the formation of a tubular network containing both the GFP-CI-MPR and the transferrin receptor (unpublished data). The statistical analyses shown in Table 1 indicate that the number of tubules growing from the TGN with an average speed of 0.9 μm/s was largely increased in BFA-treated cells. On average, BFA-treated cells could form three times more tubules than untreated cells. Furthermore, these BFA-induced tubules were more stable (duration time of 96 s) and longer (average length of 14 μm) than in untreated cells because they could not break into smaller elements. These long tubules also exhibited a tendency to form highly dynamic branched structures at their tips. The fluorescence intensity of these tubules usually increased with time, probably reflecting the free diffusion of the GFP-CI-MPR in these tubular structures, which otherwise would have been kept retained in the TGN. As expected from previous studies (Lippincott-Schwartz *et al.*, 1990), the BFA-induced formation of tubules was prevented by the addition of nocodazole, the microtubule-disrupting agent (unpublished data). Thus, the treatment of cells with BFA results in an enhanced formation and in a higher stability of tubular elements growing from the TGN. Altogether, these results indicates that the formation of TGN-derived tubules is controlled by the ARF-1 GTPase. By contrast, the treatment of GFP-CI-MPR–expressing cells with wortmannin, an inhibitor of PI-3-kinases shown to affect lysosomal enzyme sorting in mammalian cells (Brown *et al.*, 1995; Davidson, 1995), did not significantly modify the dynamics of the TGN-derived tubular elements (Table 1). Thus, the growth of TGN-derived tubules is probably not regulated by wortmannin-sensitive PI-3 kinases.

Fate of the TGN-derived Tubules

The time-lapse sequences illustrate the saltatory movement of fluorescently labeled TGN-derived tubular elements

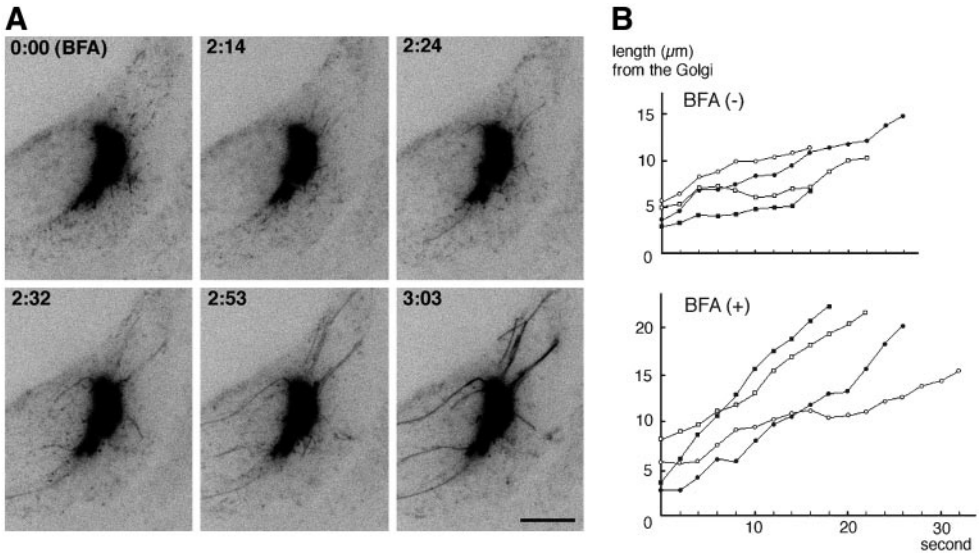

Figure 3. Effect of brefeldin A. (A) Images of GFP-CI-MPR–expressing cells were taken at 2-s time intervals during BFA treatment. Inverted images at the indicated time intervals (min:sec) are presented. The first frame (0:00) shows the cell immediately after adding BFA. Bar, 10 μm. (B) Growth of tubular elements in the absence (BFA−) or the presence (BFA+) of brefeldin A. Four examples of growing TGN tubules are shown.

along microtubules toward the cell periphery (Figures 2 and 4). However, some of these detached tubular processes sometimes reversed directions, suggesting that they could occasionally fuse back with the TGN. Therefore, we examined in more detail the fate of these GFP-labeled tubules emanating from the TGN. Figure 4 shows a video sequence taken at three frames/s of a tubular element detaching from the TGN, moving toward the cell periphery, remaining stationary for a few seconds and then mixing with other small peripheral structures also labeled with the GFP-CI-MPR. The resulting structure was also very dynamic. It rapidly fragmented into two smaller elements that fused back again. Finally, the resulting GFP-labeled structure underwent fragmentation to give rise to two distinct structures (one vesicular and another more tubular) moving toward different directions. These peripheral structures labeled with GFP are also very dynamic elements. The fast recording presented in Figure 4B shows that they could make contacts between each other, probably reflecting fusion events, before fragmenting into separate structures. This observation could support the notion that they form a dynamic network continuously fusing and breaking in order to mix/exchange their content. We then asked whether these peripheral, GFP-labeled structures were dynamically connected with endocytic compartments. To visualize this, HeLa cells were allowed to internalize for 10–15 min Alexa594-transferrin bound to the cell surface. Figure 4C shows GFP-CI-MPR-containing tubular elements and transferrin-positive structures establishing tight contacts, giving rise to structures in which the two fluorescent markers overlap. Within a few seconds, the two markers segregate again, each being packaged into separate structures. Thus, these data strongly suggest that the TGN-detached tubules can fuse with peripheral GFP-CI-MPR– containing structures and that these latter structures can exchange their content with endocytic compartments containing internalized transferrin.

Dynamics of AP-1 Coats

The results described above prompted us to investigate whether the GFP-labeled tubular elements forming at the TGN could contain the machinery required for MPR sorting, in particular the AP-1 coat whose function in MPR trafficking remains unclear at present.

GFP-CI-MPR–expressing cells were first labeled with antibodies against the γ-subunit of AP-1 or against clathrin and examined by confocal microscopy. Figure 5 shows that many GFP-labeled tubules could be decorated with anti–AP-1 and anticlathrin antibodies. It is worth noting however that AP-1 as well as clathrin do not distribute uniformly over the tubules but are detected on domains that appear to contain higher amounts of GFP-CI-MPR. As expected, AP-1 was also detected on the TGN as well as on several of the peripheral structures containing the GFP-CI-MPR (Figure 5, A and C). Second, a CFP-CI-MPR and a γ-subunit of AP-1 fused to YFP were coexpressed in HeLa cells. This γ-subunit of AP-1 fused to YFP was incorporated into a complex (unpublished data) able to bind to membranes in vivo (Figure 6A).

Western blotting experiments (unpublished data) indicated that the YFP-tagged AP-1 was distributed between a cytosolic pool (60% of total) and a membrane-bound pool (40% of total) as the endogenous AP-1. The YFP-AP-1 bound to membranes became soluble upon BFA-treatment (Figure 6B). Overall, this YFP-AP-1 exhibited a similar distribution over the TGN and peripheral, tubular structures containing internalized transferrin, as the endogenous AP-1, and was detected in membrane domains also coated with clathrin (Figure 6C). Altogether, the data strongly suggest that the YFP tag on AP-1 γ-subunit does not affect the membrane binding properties of AP-1 or its interaction with clathrin. HeLa cells coexpressing CFP-CI-MPR and YFP-AP-1 were then examined using time-lapse confocal microscopy to investigate the dynamics of both AP-1 and CI-MPR in living cells.

Several types of events could be seen as illustrated in Figure 7. First, small tubular elements coated with YFP-AP-1 and containing the CFP-CI-MPR detached from the TGN and moved toward the cell periphery. This is in good agreement with the results reported by Sorkin and coworkers (Huang *et al.*, 2001). Frequently, the YFP-AP-1 coat did not seem to be uniformly distributed along these tubular elements but appeared as patches moving along CFP-CI-MPR–labeled tubules as seen for the endogenous AP-1 in fixed cells (Figure 5A). Occasionally, TGN-derived tubules containing the CFP-CI-MPR moving toward the cell periphery appeared to lose their YFP-AP-1 coat. In other cases however, this coat remained associated with these structures, which could nevertheless fuse with peripheral tubular structures. As reported earlier, the YFP-AP-1 coated, CFP-CI-MPR–containing peripheral tubular structures appeared as highly dynamic structures. Although they were partly coated with YFP-AP-1, these structures could ultimately fuse with each other. It should be noted, however, that some tubular elements forming at the TGN appeared to be devoid of the YFP-AP-1 complex. The quantification indicates that 35% of the CFP-CI-MPR–containing tubules are devoid of YFP-AP-1 when they detach from the TGN. As shown in Figure 7, some of these tubules could acquire an YFP-AP-1 coat while they move toward the cell periphery. Altogether, these data show that AP-1 is present on structures where sorting of CI-MPR occurs, i.e., TGN and peripheral elements, probably endosomes as well as on transport intermediates carrying the CI-MPR.

DISCUSSION

In this study, we have used fluorescence time-lapse imaging of GFP fused to the transmembrane and cytoplasmic domains of the CI-MPR in order to study its trafficking in living cells. As schematically represented in Figure 8, high-resolution imaging of the Golgi region shows that tubular processes containing the GFP-CI-MPR pull off, detach from the TGN, and occasionally fragment into smaller tubular elements. These detached elements make contacts, probably fusing, with peripheral tubulo-vesicular structures also containing small amounts of GFP-CI-MPR. These structures appear to form a dynamic, discontinuous, post-TGN network able to fuse with early endocytic compartments. Two color imaging of living cells indicates that the AP-1 complex is present on many TGN-derived tubules, thereby suggesting that AP-1 may participate, as GGAs, in this sorting and transport process.

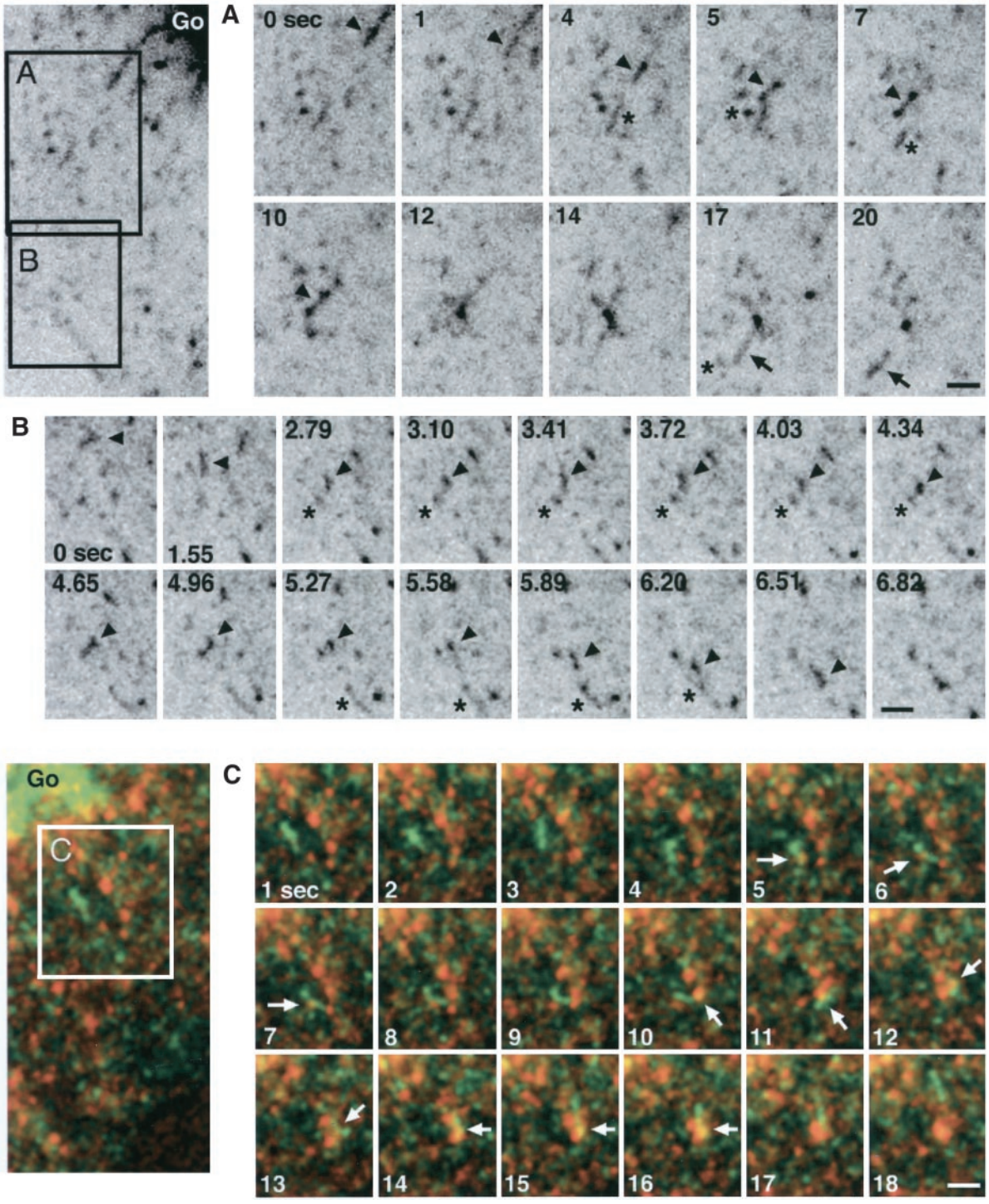

Figure 4. Fate of tubular elements detaching from the TGN. (A) TGN-derived tubular elements mix with GFP-labeled peripheral structures. An area of a GFP-CI-MPR–expressing HeLa cell was selected as indicated in the left panel and examined by videomicroscopy. Images were taken at a high speed (3 frames per second). Inverted images are presented. Sequences of images taken at the indicated time intervals are displayed in B. The arrow indicates a tubular element detaching from a TGN tubule and fusing with a peripheral compartment labeled with the GFP. (B) GFP-labeled, peripheral structures are highly dynamic. Cells were examined as in A. The arrow and the asterisk indicate different peripheral structures containing the GFP-CI-MPR. (C) Mixing of GFP-CI-MPR–positive structures with endocytic compartments. GFP-CI-MPR–expressing cells were incubated at 4°C with Alexa594-transferrin for 30 min and then washed and reincubated at 37°C for 10–15 min. The cells were examined by confocal microscopy. Images were recorded every second. The arrow indicates the overlap between the two fluorescent markers. Bar, 2 μm.

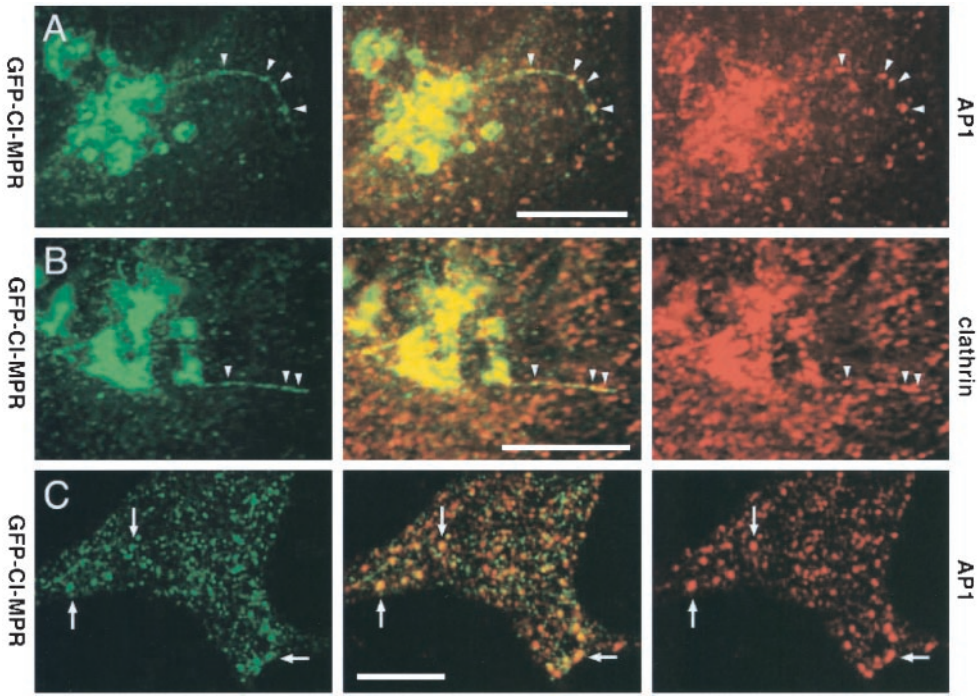

Figure 5. Distribution of endogenous coat components. (A–C) HeLa cells expressing GFP-CI-MPR (green) were fixed, labeled with either the 100.3 mAb against γ-adaptin (red; AP-1; A and C) or a polyclonal antibody against clathrin (red; B), and examined by laser confocal microscopy. (A and B) the signals in the Golgi region; (C) signals in the periphery of the cell. Note that AP-1 or clathrin signals appear as concentrated spots along the TGN tubules (arrowheads).

Export of GFP-CI-MPR from the Secretory Pathway

Our study based on time-lapse imaging of GFP-CI-MPR first suggests that MPRs are sorted into tubular elements of various lengths rather than in vesicles similar to endocytic clathrin-coated vesicles. We made similar observations with GFP fused to the transmembrane and cytoplasmic domains of the CD-MPR or those of the gpI envelope protein of the varicella-zoster virus, a TGN marker trafficking like the MPRs (Alconada *et al.*, 1996). It is unlikely that the formation of these tubular elements is due to the presence of large aggregates of GFP-CI-MPRs because cross-linking experiments using membrane permeable agents indicated that GFP-CI-MPRs are found in membranes as monomers (unpublished data). Our measurements indicate that the surface area of membranes sorted by this tubule-dependent mechanism could correspond to that of ≈200 typical clathrin-coated vesicles formed per minute, assuming that tubules have the same diameter as vesicles. In cultured cells, ≈1600 clathrin-coated vesicles are formed per minute during endocytosis (Marsh and Helenius, 1980), a pathway that is by far more dynamic than TGN to endosome transport. In addition, measurements of the fluorescence intensity of these tubular elements indicate that ≈2% of the intracellular GFP-CI-MPR could be sorted every minute along this tubular pathway. Thus, the bulk of the GFP-CI-MPR contained in the TGN could be exported within 50 min. Thus, these TGN-derived tubules could substantially contribute for sorting of MPRs from the secretory pathway. It is likely that such transport intermediates cannot be recovered in typical preparations of clathrin-coated vesicles because the various methods used select transport intermediates with an average size of ≈150 nm and a high density. It is also possible that such tubular structures are fragile and yield vesicles upon cell breakage.

Several studies have also highlighted the potential role of tubules in membrane traffic, especially in transport of membrane proteins from the Golgi complex back to the endoplasmic reticulum (Sciaky *et al.*, 1997; White *et al.*, 1999) or from the Golgi to the plasma membrane (Hirschberg *et al.*, 1998; Nakata *et al.*, 1998; Toomre *et al.*, 1999). In living cells, the GFP-KDEL receptor is detected inside membrane tubules detaching from Golgi structures and moving along microtubule tracks. Brefeldin A treatment accentuates tubule formation without detachment. Similarly, GFP-tagged VSV-G protein en route to the cell surface is detected in long tubular structures that detach from the Golgi and rapidly fuse with the plasma membrane without intersecting other membrane pathways (Hirschberg *et al.*, 1998; Toomre *et al.*, 1999).

Dynamics of TGN-derived Tubules

The dynamic state of the TGN-derived tubules is regulated by several factors. The first one is the ARF-1 GTPase. Although ARF-1 regulates the interaction of several coat components with Golgi membranes (for review see Schekman and Orci, 1996), it also activates enzymes such as phospholipase D (for review see Roth *et al.*, 1999) or kinases involved in phosphoinositide metabolism (Godi *et al.*, 1999). Therefore, it cannot be excluded that this GTPase, independently of its activity in coat recruitment, also regulates the activity of other molecules involved in the tubule growth process.

Second, the formation and the movement of the GFP-CI-MPR–containing tubules require intact microtubules. If the detached tubules exhibit a stochastic movement, they move toward the cell periphery with an average maximal speed of 1 μm/s, suggesting that kinesin-like motors are involved in their plus-end directed movement. This would be consistent

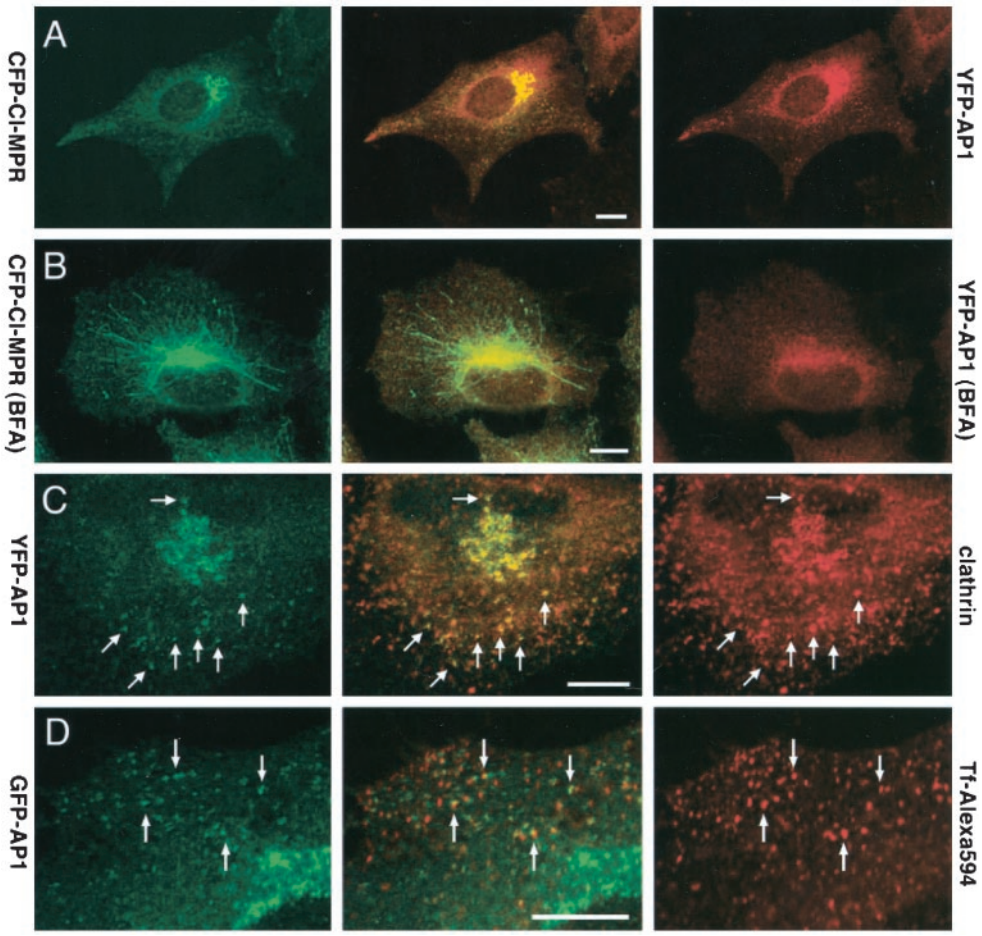

Figure 6. Steady state distribution of YFP-tagged γ-adaptin. (A and B) HeLa cells expressing both CFP-CI-MPR (green) and YFP-γ-adaptin (red; YFP-AP1) were treated without (A) or with BFA (B) for 10 min and fixed. (C) Hela cells expressing YFP-γ-adaptin (green) were also labeled with antibodies against clathrin (red). (D) HeLa cells expressing GFP-γ-adaptin (green; GFP-AP1) were allowed to internalize Alexa594-labeled transferrin for 10 min at 37°C (red; Tf-Alexa594). Merged images are presented in the middle column. Bars, 10 μm

with previous studies showing that the disruption of microtubules with nocodazole impairs lysosomal enzyme transport to endocytic compartments (Scheel *et al.*, 1990). The kinesin KIF-13A that has been shown to be involved in MPR transport from TGN (Nakagawa *et al.*, 2000) could be a candidate for the kinesin involved in the growth of TGN-derived tubules.

The actin network also appears to play some role in the formation of TGN-derived tubules containing the GFP-CI-MPR, as illustrated by the cytochalasin D effect. The role of actin in this growth process is not clear. Several lines of evidence link endocytosis with the actin network both in yeast (for review see Wendland *et al.*, 1998) and mammalian cells (Gottlieb *et al.*, 1993; Durrbach *et al.*, 1996; Lamaze *et al.*, 1997). Time-lapse imaging of endocytic clathrin-coated pits and vesicles has further highlighted the involvement of an actin-based framework in endocytosis (Gaidarov *et al.*, 1999). Clathrin-coated pits are not randomly distributed within the plasma membrane. They show definite, but highly limited mobility, a phenomenon that is relaxed upon cell treatment with latrunculin D, an inhibitor of actin assembly. We also observed that tubule formation is not a random phenomenon but appears to be restricted to preferential sites on TGN membranes. Although this suggests that actin could fulfill a similar function at the TGN, it is likely that actin plays some additional role in the growth of TGN-derived tubules because this process is totally impaired in the absence of an actin network, whereas budding of endocytic clathrin-coated vesicles is not.

Fate of TGN-derived Tubules

Our time-lapse videomicroscopy illustrates that TGN-derived tubules intersect with peripheral structures that also contain GFP-CI-MPR. Direct fusion between TGN-derived tubules and plasma membrane as seen during direct transport from TGN to plasma membrane (Hirschberg *et al.*, 1998; Toomre *et al.*, 1999), although occasionally detectable, was extremely rare. Our time-lapse imaging also shows that these peripheral structures are highly dynamic, most likely forming a post-TGN network whose different elements are continuously fusing with each other and breaking into separate elements. This network is dynamically connected with early endocytic compartments because several of its elements can fuse with endosomes labeled with internalized transferrin. We found that ≈20–30% of the elements forming this peripheral network also contain endocytosed transferrin at any given time. Such a dynamic state would probably facilitate the rapid mixing and sorting of endosomal membrane proteins. It is also interesting to note that, after

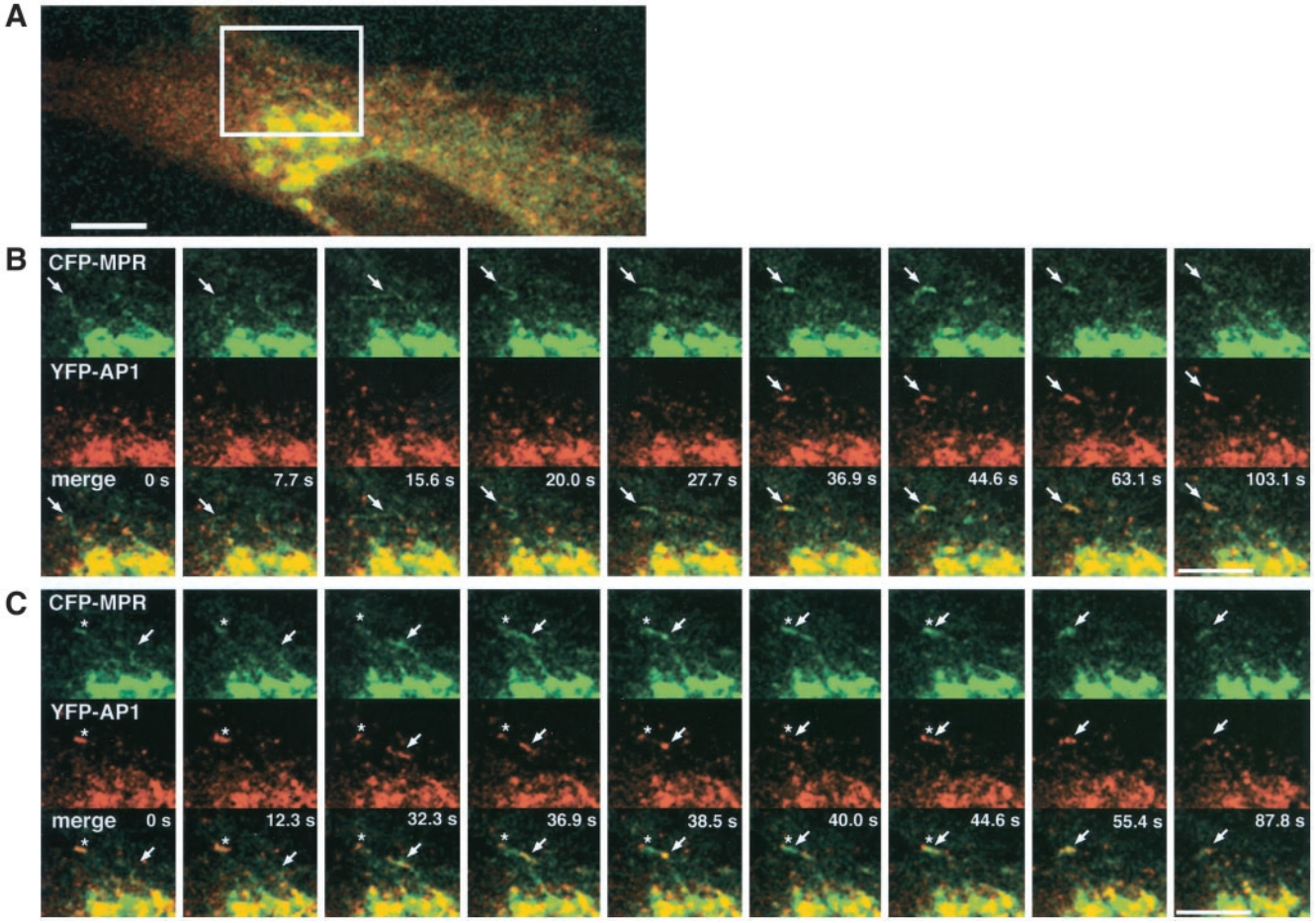

Figure 7. Dynamics of YFP-AP-1 and CFP-CI-MPR. HeLa cells expressing both CFP-CI-MPR (green) and YFP-γ-adaptin (red; YFP-AP1) were observed by time-lapse laser scanning microscopy. Images were taken every 1.5 s with multitrack mode. A selected area indicated in A is displayed in B and C at the time intervals as indicated. Merged images are shown at the bottom. (B) A TGN-derived tubular element (arrow) without any AP1-coat moves toward the periphery and acquires an AP1-coat. (C) Another tubular element with an AP1-coat (arrow) detaches from the TGN and appears to fuse with the peripheral compartment (asterisk) that has been formed in B. Bars, 10 μm.

fusion the GFP-CI-MPR segregates away from the transferrin bound to its receptor. This suggests that, after fusion these two transmembrane proteins can be clustered into two different membrane domains giving rise to two distinct elements after fission.

Although the peripheral tubular network visualized in this study using GFP-CI-MPR remains to be better characterized, it is reminiscent to the tubular endosomal network distinct from late endosomes described earlier by Tooze and Hollinshead (1991) or by Hopkins and colleagues (Hopkins *et al.*, 1990). The relatively long time required to fill-up this entire tubular network with a fluid phase marker (≈30 min) suggests that their interactions with "classical" early endosomes are transient, as observed in our study using time-lapse microscopy. We believe that the pathway followed by GFP-CI-MPR reflects that of the endogenous MPRs en route from the TGN to endosomes. Our study in living cells would therefore strengthen the notion that the secretory pathway is connected with early endocytic compartments. This interpretation would be consistent with previous studies showing that newly synthesized lysosomal enzymes are present in early endocytic compartments of mammalian cells (Ludwig *et al.*, 1991) where they can accumulate together with the MPRs when transport from early to late endocytic compartments is impaired (Press *et al.*, 1998). Whether, these TGN-derived tubules can also fuse with late endocytic compartments remains, however, to be determined.

MPR Trafficking and AP-1 Coats

The GGA proteins interact with acidic cluster-dileucine based sorting motifs of the MPR tails (Puertollano *et al.*, 2001b; Zhu *et al.*, 2001). These motifs are essential for lysosomal enzyme targeting. Furthermore, GGA1 is clearly detected on TGN-derived transport intermediates carrying the cation-dependent mannose 6-phosphate receptor (Puertollano *et al.*, 2001a), clearly indicating that GGAs are involved in MPR sorting in the TGN. Conversely, the inactivation of their homologues (Gga1p and Gga2p) in yeast leads to a missorting of vacuolar enzymes as well as a defect in alpha-

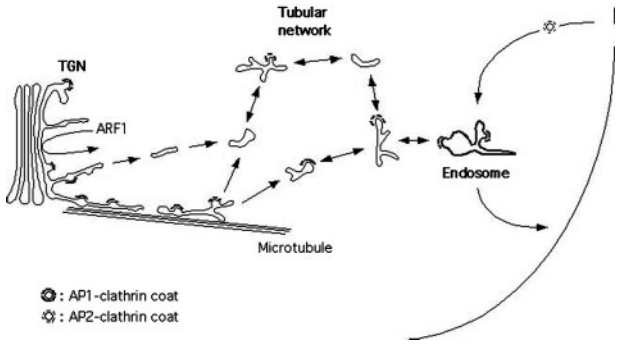

Figure 8. Schematic representation of MPR transport. In this model, tubular elements, containing the GFP-CI-MPR and partly coated with AP-1 and clathrin patches, detach from the TGN, and fuse with peripheral tubulo-vesicular structures also containing this marker. These structures rapidly fuse with each others probably forming a highly dynamic network whose various separate elements make contact with early endocytic structures. Typical clathrin-coated vesicles, as purified using classical methods, could represent a subpopulation of these tubulo-vesicular transport intermediates selected for their size and high density. It is also possible that these tubulo-vesicular transport intermediates are fragile and yield vesicles upon cell breakage.

factor processing (Hirst *et al.*, 2001; Mullins and Bonifacino, 2001). Our study shows that AP-1 is also detected on TGN-derived tubules containing GFP-CI-MPR chimera. It should be noted however that AP-1 does not distribute uniformly over the length of the tubules but is rather detected on discrete areas in which GFP-CI-MPR chimera appear to be more concentrated. Thus, this data would suggest that AP-1 functions, as GGAs, in MPR sorting from the TGN. AP-1 binding to membranes requires acidic clusters in the CD-MPR tail (Mauxion *et al.*, 1996), a process that could also involve PACS proteins (Wan *et al.*, 1998). Tyrosine-based sorting signals also facilitate lysosomal enzyme targeting to lysosomes (Jadot *et al.*, 1992), probably by interacting with the AP-1 μ chain (Bonifacino and Dell'Angelica, 1999). Whether, AP-1 and GGAs function along the same sorting pathway in mammalian cells or in parallel pathways to package MPRs as well as other trans-membrane proteins in distinct transport carriers destined to different compartments remains to be determined.

Some of the TGN-derived tubules carrying the CFP-CI-MPR were not labeled with YFP-AP-1. Whether, this reflects a low abundance of AP-1, below the limit of detection, or a real lack of AP-1 coat remains to be determined. In yeast, the disruption of genes encoding either Gga2 or AP-1 beta-subunit (ALP2) gene alone has no drastic effect and cells are phenotypically normal. However, cells carrying both null mutations are defective in growth, alpha-factor maturation, and transport of carboxypeptidase S to the vacuole (Costaguta *et al.*, 2001). Furthermore, disruption of both GGA genes and APL2 results in cells severely compromised in growth. These results could suggest that GGAs and AP-1 have overlapping sorting functions. However, Pep12p, a yeast syntaxin located in late endosomes, becomes mislocalized in early endosomes in strains lacking Gga1p and Gga2p, suggesting that GGA proteins help create vesicles destined for late endosomes (Black and Pelham, 2000). Our study in mammalian cells shows that TGN-derived transport intermediates coated with AP-1 fuse with peripheral structures dynamically connected with early endosomes. Thus, double imaging of GFP-labeled GGAs and AP-1 could potentially shed some light on their precise sorting functions.

AP-1 is not only present on the TGN but also on endosomal membranes (Le Borgne *et al.*, 1996; Futter *et al.*, 1998), as also illustrated in this study. In a similar manner, clathrin coats have been detected on tubular endocytic structures. These clathrin coats have been involved in the recycling pathway to the plasma membrane (Stoorvogel *et al.*, 1987; van Dam and Stoorvogel, 2002) or in transport to lysosomes (Sachse *et al.*, 2002). Endosomal AP-1 has been involved in the polarized distribution of the transferrin receptor in polarized cells (Futter *et al.*, 1998). More recently, AP-1 has been proposed to mediate the retrograde transport of membrane proteins back to the TGN. Mammalian cells carrying an inactivated μ1-A gene are less efficient for retrieval of CD-MPR back to the Golgi and as a consequence accumulate MPRs in early endosomes (Meyer *et al.*, 2000). Similarly in yeast, disruption of AP-1 restores transport to the plasma membrane of Chitin synthase III, which otherwise populates an intracellular reservoir that is maintained by a cycle of transport between the TGN and early endosomes (Valdivia *et al.*, 2002). However, these studies do not totally exclude the possibility that AP-1 functions in TGN sorting. Our study using time-lapse microscopy could suggest that AP-1 on endosomes could maintain transmembrane proteins, i.e., the MPRs within membrane microdomains of the peripheral tubular network that we describe in this study and restricts their access to the early endosomal system or to the cell surface. In the absence of functional AP-1, the MPRs would become more concentrated in early endocytic compartments, and therefore could recycle more frequently between early endosomes and the cell surface than they would from endosomes back to the TGN. This is precisely the phenotype of mammalian cells carrying an inactivated μ1-A gene (Meyer *et al.*, 2000).

ACKNOWLEDGMENTS

We thank Drs. P. Chardin, E. Karsenti, P. Mangeat and T. Nilsson for kindly providing us with antibodies or cDNAs; Dr Zerial for critical reading of the manuscript; and members of Hoflack's and Uchiyama's laboratories for helpful discussions. This work is supported by grants from the CNRS, ARC, the Region Nord-Pas de Calais, and Japan Ministry of Education, Culture, Sports, Science and Technology (a Grant-in-Aid for Scientific Research on Priority Areas (C)-Advanced Brain Science Project). S.W. was supported by fellowships from Japan Ministry of Education, Culture, Science, Sports, Science, and Technology, from Japan Society for the promotion of Science and from the Region Nord-Pas de Calais.

REFERENCES

Alconada, A., Bauer, U., and Hoflack, B. (1996). A tyrosine-based motif and a casein kinase II phosphorylation site regulate the intracellular trafficking of the varicella-zoster virus glycoprotein I, a protein localized in the trans-Golgi network. EMBO J. *15*, 6096–6110.

Bell, G.I., Santerre, R.F., and Mullenbach, G.T. (1983). Hamster preproglucagon contains the sequence of glucagon and two related peptides. Nature *302*, 716–718.

Black, M.W., and Pelham, H.R. (2000). A selective transport route from Golgi to late endosomes that requires the yeast GGA proteins. J. Cell Biol. *151*, 587–600.

Bock, J.B., Klumperman, J., Davanger, S., and Scheller, R.H. (1997). Syntaxin 6 functions in trans-Golgi network vesicle trafficking. Mol. Biol. Cell *8*, 1261–1271.

Boman, A.L., Zhang, C., Zhu, X., and Kahn, R.A. (2000). A family of ADP-ribosylation factor effectors that can alter membrane transport through the trans-Golgi. Mol. Biol. Cell *11*, 1241–1255.

Bonifacino, J.S., and Dell'Angelica, E.C. (1999). Molecular bases for the recognition of tyrosine-based sorting signals. J. Cell Biol. *145*, 923–926.

Brown, W.J., DeWald, D.B., Emr, S.D., Plutner, H., and Balch, W.E. (1995). Role for phosphatidylinositol 3-kinase in the sorting and transport of newly synthesized lysosomal enzymes in mammalian cells. J. Cell Biol. *130*, 781–796.

Canfield, W.M., Johnson, K.F., Ye, R.D., Gregory, W., and Kornfeld, S. (1991). Localization of the signal for rapid internalization of the bovine cation-independent mannose 6-phosphate/insulin-like growth factor-II receptor to amino acids 24–29 of the cytoplasmic tail. J. Biol. Chem. *266*, 5682–5688.

Chen, H.J., Remmler, J., Delaney, J.C., Messner, D.J., and Lobel, P. (1993). Mutational analysis of the cation-independent mannose 6-phosphate/insulin-like growth factor II receptor. A consensus casein kinase II site followed by 2 leucines near the carboxyl terminus is important for intracellular targeting of lysosomal enzymes. J. Biol. Chem. *268*, 22338–22346.

Costaguta, G., Stefan, C.J., Bensen, E.S., Emr, S.D., and Payne, G.S. (2001). Yeast Gga coat proteins function with clathrin in Golgi to endosome transport. Mol. Biol. Cell. *12*, 1885–1896.

Davidson, H.W. (1995). Wortmannin causes mistargeting of procathepsin D. Evidence for the involvement of a phosphatidylinositol 3-kinase in vesicular transport to lysosomes. J. Cell Biol. *130*, 797–805.

Dell'Angelica, E.C., Puertollano, R., Mullins, C., Aguilar, R.C., Vargas, J.D., Hartnell, L.M., and Bonifacino, J.S. (2000). GGAs: a family of ADP ribosylation factor-binding proteins related to adaptors and associated with the Golgi complex. J. Cell Biol. *149*, 81–94.

Durrbach, A., Louvard, D., and Coudrier, E. (1996). Actin filaments facilitate two steps of endocytosis. J. Cell Sci. *109*, 457–465.

Folsch, H., Pypaert, M., Schu, P., and Mellman, I. (2001). Distribution and function of AP-1 clathrin adaptor complexes in polarized epithelial cells. J. Cell Biol. *152*, 595–606.

Futter, C.E., Gibson, A., Allchin, E.H., Maxwell, S., Ruddock, L.J., Odorizzi, G., Domingo, D., Trowbridge, I.S., and Hopkins, C.R. (1998). In polarized MDCK cells basolateral vesicles arise from clathrin-gamma- adaptin-coated domains on endosomal tubules. J. Cell Biol. *141*, 611–623.

Gaidarov, I., Santini, F., Warren, R.A., and Keen, J.H. (1999). Spatial control of coated-pit dynamics in living cells. Nat Cell Biol *1*, 1–7.

Geuze, H.J., Slot, J.W., Strous, G.J., Hasilik, A., and von Figura, K. (1985). Possible pathways for lysosomal enzyme delivery. J. Cell Biol. *101*, 2253–2262.

Godi, A., Pertile, P., Meyers, R., Marra, P., Di Tullio, G., Iurisci, C., Luini, A., Corda, D., and De Matteis, M.A. (1999). ARF mediates recruitment of PtdIns-4-OH kinase-beta and stimulates synthesis of PtdIns(4,5)P2 on the Golgi complex. Nat. Cell Biol. *1*, 280–287.

Gottlieb, T.A., Ivanov, I.E., Adesnik, M., and Sabatini, D.D. (1993). Actin microfilaments play a critical role in endocytosis at the apical but not the basolateral surface of polarized epithelial cells. J. Cell Biol. *120*, 695–710.

Hirschberg, K., Miller, C.M., Ellenberg, J., Presley, J.F., Siggia, E.D., Phair, R.D., and Lippincott-Schwartz, J. (1998). Kinetic analysis of secretory protein traffic and characterization of golgi to plasma membrane transport intermediates in living cells. J. Cell Biol. *143*, 1485–1503.

Hirst, J., Lindsay, M.R., and Robinson, M.S. (2001). GGAs: roles of the different domains and comparison with AP-1 and clathrin. Mol. Biol. Cell *12*, 3573–3588.

Hirst, J., Lui, W.W., Bright, N.A., Totty, N., Seaman, M.N., and Robinson, M.S. (2000). A family of proteins with gamma-adaptin and VHS domains that facilitate trafficking between the trans-Golgi network and the vacuole/lysosome. J. Cell Biol. *149*, 67–80.

Hopkins, C.R., Gibson, A., Shipman, M., and Miller, K. (1990). Movement of internalized ligand-receptor complexes along a continuous endosomal reticulum. Nature *346*, 335–339.

Huang, F., Nesterov, A., Carter, R.E., and Sorkin, A. (2001). Trafficking of yellow-fluorescent-protein-tagged mu1 subunit of clathrin adaptor AP-1 complex in living cells. Traffic *2*, 345–357.

Jadot, M., Canfield, W.M., Gregory, W., and Kornfeld, S. (1992). Characterization of the signal for rapid internalization of the bovine mannose 6-phosphate/insulin-like growth factor-II receptor. J. Biol. Chem. *267*, 11069–11077.

Johnson, K.F., and Kornfeld, S. (1992a). The cytoplasmic tail of the mannose 6-phosphate/insulin-like growth factor-II receptor has two signals for lysosomal enzyme sorting in the Golgi. J. Cell Biol. *119*, 249–257.

Johnson, K.F., and Kornfeld, S. (1992b). A His-Leu-Leu sequence near the carboxyl terminus of the cytoplasmic domain of the cation-dependent mannose 6-phosphate receptor is necessary for the lysosomal enzyme sorting function. J. Biol. Chem. *267*, 17110–17115.

Klausner, R.D., Donaldson, J.G., and Lippincott-Schwartz, J. (1992). Brefeldin A: insights into the control of membrane traffic and organelle structure. J. Cell Biol. *116*, 1071–1080.

Klumperman, J., Kuliawat, R., Griffith, J.M., Geuze, H.J., and Arvan, P. (1998). Mannose 6-phosphate receptors are sorted from immature secretory granules via adaptor protein AP-1, clathrin, and syntaxin 6-positive vesicles. J. Cell Biol. *141*, 359–371.

Kornfeld, S. (1992). Structure and function of the mannose 6-phosphate/insulinlike growth factor II receptors. Annu. Rev. Biochem. *61*, 307–330.

Lamaze, C., Fujimoto, L.M., Yin, H.L., and Schmid, S.L. (1997). The actin cytoskeleton is required for receptor-mediated endocytosis in mammalian cells. J. Biol. Chem. *272*, 20332–20335.

Le Borgne, R., Griffiths, G., and Hoflack, B. (1996). Mannose 6-phosphate receptors and ADP-ribosylation factors cooperate for high affinity interaction of the AP-1 Golgi assembly proteins with membranes. J. Biol. Chem. *271*, 2162–2170.

Lippincott-Schwartz, J., Donaldson, J.G., Schweizer, A., Berger, E.G., Hauri, H.P., Yuan, L.C., and Klausner, R.D. (1990). Microtubule-dependent retrograde transport of proteins into the ER in the presence of brefeldin A suggests an ER recycling pathway. Cell *60*, 821–836.

Lippincott-Schwartz, J., Yuan, L., Tipper, C., Amherdt, M., Orci, L., and Klausner, R.D. (1991). Brefeldin A's effects on endosomes, lysosomes, and the TGN suggest a general mechanism for regulating organelle structure and membrane traffic. Cell *67*, 601–616.

Ludwig, T., Griffiths, G., and Hoflack, B. (1991). Distribution of newly synthesized lysosomal enzymes in the endocytic pathway of normal rat kidney cells. J. Cell Biol. *115*, 1561–1572.

Ludwig, T., Le Borgne, R., and Hoflack, B. (1995). Roles for mannose 6-phosphate receptors in lysosomal enzyme sorting, IGF-II binding and clathrin-coat assembly. Trends Cell Biol. *5*, 202–206.

Marsh, M., and Helenius, A. (1980). Adsorptive endocytosis of Semliki Forest virus. J. Mol. Biol. *142*, 439–454.

Mauxion, F., Le Borgne, R., Munier-Lehmann, H., and Hoflack, B. (1996). A casein kinase II phosphorylation site in the cytoplasmic domain of the cation-dependent mannose 6-phosphate receptor determines the high affinity interaction of the AP-1 Golgi assembly proteins with membranes. J. Biol. Chem. *271*, 2171–2178.

Mellman, I. (1996). Endocytosis and molecular sorting. Annu. Rev. Cell Dev. Biol. *12*, 575–625.

Meyer, C., Zizioli, D., Lausmann, S., Eskelinen, E.L., Hamann, J., Saftig, P., von Figura, K., and Schu, P. (2000). Mu1A-adaptin-deficient mice: lethality, loss of AP-1 binding and rerouting of mannose 6-phosphate receptors. EMBO J. *19*, 2193–203.

Mullins, C., and Bonifacino, J.S. (2001). Structural requirements for function of yeast GGAs in vacuolar protein sorting, alpha-factor maturation, and interactions with clathrin. Mol. Cell. Biol. *21*, 7981–7994.

Nakagawa, T., Setou, M., Seog, D., Ogasawara, K., Dohmae, N., Takio, K., and Hirokawa, N. (2000). A novel motor, KIF13A, transports mannose-6-phosphate receptor to plasma membrane through direct interaction with AP-1 complex. Cell *103*, 569–581.

Nakata, T., Terada, S., and Hirokawa, N. (1998). Visualization of the dynamics of synaptic vesicle and plasma membrane proteins in living axons. J. Cell Biol. *140*, 659–674.

Nielsen, M.S., Madsen, P., Christensen, E.I., Nykjaer, A., Gliemann, J., Kasper, D., Pohlmann, R., and Petersen, C.M. (2001). The sortilin cytoplasmic tail conveys Golgi-endosome transport and binds the VHS domain of the GGA2 sorting protein. EMBO J. *20*, 2180–2190.

Press, B., Feng, Y., Hoflack, B., and Wandinger-Ness, A. (1998). Mutant Rab7 causes the accumulation of cathepsin D and cation-independent mannose 6-phosphate receptor in an early endocytic compartment. J. Cell Biol. *140*, 1075–1089.

Puertollano, R., Aguilar, R.C., Gorshkova, I., Crouch, R.J., and Bonifacino, J.S. (2001a). Sorting of mannose 6-phosphate receptors mediated by the GGAs. Science *292*, 1712–1716.

Puertollano, R., Randazzo, P.A., Presley, J.F., Hartnell, L.M., and Bonifacino, J.S. (2001b). The GGAs promote ARF-dependent recruitment of clathrin to the TGN. Cell *105*, 93–102.

Rabouille, C., Hui, N., Hunte, F., Kieckbusch, R., Berger, E.G., Warren, G., and Nilsson, T. (1995). Mapping the distribution of Golgi enzymes involved in the construction of complex oligosaccharides. J. Cell Sci. *108*, 1617–1627.

Robinson, M.S., and Bonifacino, J.S. (2001). Adaptor-related proteins. Curr. Opin. Cell Biol. *13*, 444–453.

Robinson, M.S., and Kreis, T.E. (1992). Recruitment of coat proteins onto Golgi membranes in intact and permeabilized cells: effects of brefeldin A and G protein activators. Cell *69*, 129–138.

Roth, M.G., Bi, K., Ktistakis, N.T., and Yu, S. (1999). Phospholipase D as an effector for ADP-ribosylation factor in the regulation of vesicular traffic. Chem. Phys. Lipids *98*, 141–152.

Sachse, M., Urbe, S., Oorschot, V., Strous, G.J., and Klumperman, J. (2002). Bilayered clathrin coats on endosomal vacuoles are involved in protein ;Sorting toward lysosomes. Mol. Biol. Cell. *13*, 1313–1328.

Scheel, J., Matteoni, R., Ludwig, T., Hoflack, B., and Kreis, T.E. (1990). Microtubule depolymerization inhibits transport of cathepsin D from the Golgi apparatus to lysosomes. J. Cell Sci. *96*, 711–720.

Schekman, R., and Orci, L. (1996). Coat proteins and vesicle budding. Science *271*, 1526–1533.

Schmid, S.L. (1997). Clathrin-coated vesicle formation and protein sorting: an integrated process. Annu. Rev. Biochem. *66*, 511–548.

Schweizer, A., Kornfeld, S., and Rohrer, J. (1997). Proper sorting of the cation-dependent mannose 6-phosphate receptor in endosomes depends on a pair of aromatic amino acids in its cytoplasmic tail. Proc. Natl. Acad. Sci. USA *94*, 14471–14476.

Sciaky, N., Presley, J., Smith, C., Zaal, K.J., Cole, N., Moreira, J.E., Terasaki, M., Siggia, E., and Lippincott-Schwartz, J. (1997). Golgi tubule traffic and the effects of brefeldin A visualized in living cells. J. Cell Biol. *139*, 1137–1155.

Stamnes, M.A., and Rothman, J.E. (1993). The binding of AP-1 clathrin adaptor particles to Golgi membranes requires ADP-ribosylation factor, a small GTP-binding protein. Cell *73*, 999–1005.

Stoorvogel, W., Geuze, H.J., and Strous, G.J. (1987). Sorting of endocytosed transferrin and asialoglycoprotein occurs immediately after internalization in HepG2 cells. J. Cell Biol. *104*, 1261–1268.

Takatsu, H., Katoh, Y., Shiba, Y., and Nakayama, K. (2001). Golgi-localizing, gamma-adaptin ear homology domain, ADP-ribosylation factor-binding (GGA) proteins interact with acidic dileucine sequences within the cytoplasmic domains of sorting receptors through their Vps27p/Hrs/STAM (VHS) domains. J. Biol. Chem. *276*, 28541–28545.

Toomre, D., Keller, P., White, J., Olivo, J.C., and Simons, K. (1999). Dual-color visualization of trans-Golgi network to plasma membrane traffic along microtubules in living cells. J. Cell Sci. *112*, 21–33.

Tooze, J., and Hollinshead, M. (1991). Tubular early endosomal networks in AtT20 and other cells. J. Cell Biol. *115*, 635–653.

Traub, L.M., Ostrom, J.A., and Kornfeld, S. (1993). Biochemical dissection of AP-1 recruitment onto Golgi membranes. J. Cell Biol. *123*, 561–573.

Valdivia, R.H., Baggott, D., Chuang, J.S., and Schekman, R.W. (2002). The yeast clathrin adaptor protein complex 1 is required for the efficient retention of a subset of late Golgi membrane proteins. Dev. Cell *2*, 283–294.

van Dam, E.M., and Stoorvogel, W. (2002). Dynamin-dependent transferrin receptor recycling by endosome-derived clathrin-coated vesicles. Mol. Biol. Cell *13*, 169–182.

Wan, L., Molloy, S.S., Thomas, L., Liu, G., Xiang, Y., Rybak, S.L., and Thomas, G. (1998). PACS-1 defines a novel gene family of cytosolic sorting proteins required for trans-Golgi network localization. Cell *94*, 205–216.

Wendland, B., Emr, S.D., and Riezman, H. (1998). Protein traffic in the yeast endocytic and vacuolar protein sorting pathways. Curr. Opin. Cell Biol. *10*, 513–522.

White, J. *et al.* (1999). Rab6 coordinates a novel Golgi to ER retrograde transport pathway in live cells. J. Cell Biol. *147*, 743–760.

Wong, D.H., and Brodsky, F.M. (1992). 100-kD proteins of Golgi- and trans-Golgi network-associated coated vesicles have related but distinct membrane binding properties. J. Cell Biol. *117*, 1171–1179.

Zhu, Y., Doray, B., Poussu, A., Lehto, V.P., and Kornfeld, S. (2001). Binding of GGA2 to the lysosomal enzyme sorting motif of the mannose 6-phosphate receptor. Science *292*, 1716–1718.

Zhu, Y., Drake, M.T., and Kornfeld, S. (1999). ADP-ribosylation factor 1 dependent clathrin-coat assembly on synthetic liposomes. Proc. Natl. Acad. Sci. USA *96*, 5013–5018.

Zhu, Y., Traub, L.M., and Kornfeld, S. (1998). ADP-ribosylation factor 1 transiently activates high-affinity adaptor protein complex AP-1 binding sites on Golgi membranes. Mol. Biol. Cell *9*, 1323–1337.